

FORMATION OF GLOBULAR CLUSTERS WITH INTERNAL ABUNDANCE SPREADS IN R-PROCESS ELEMENTS: STRONG EVIDENCE FOR PROLONGED STAR FORMATION

KENJI BEKKI

ICRAR, M468, The University of Western Australia 35 Stirling Highway, Crawley Western Australia, 6009, Australia

AND

TAKUJI TSUJIMOTO

National Astronomical Observatory of Japan, Mitaka-shi, Tokyo 181-8588, Japan

Draft version January 12, 2022

ABSTRACT

Several globular clusters (GCs) in the Galaxy are observed to show internal abundance spreads in r -process elements (e.g., Eu). We here propose a new scenario which explains the origin of these GCs (e.g., M5 and M15). In this scenario, stars with no/little abundance variations first form from a massive molecular cloud (MC). After all of the remaining gas of the MC is expelled by numerous supernovae, gas ejected from asymptotic giant branch stars can be accumulated in the central region of the GC to form a high-density intra-cluster medium (ICM). Merging of neutron stars then occurs to eject r -process elements, which can be efficiently trapped in and subsequently mixed with the ICM. New stars formed from the ICM can have r -process abundances quite different from those of earlier generations of stars within the GC. This scenario can explain both (i) why r -process elements can be trapped within GCs and (ii) why GCs with internal abundance spreads in r -process elements do not show [Fe/H] spreads. Our model shows that (i) a large fraction of Eu-rich stars can be seen in Na-enhanced stellar populations of GCs, as observed in M15, and (ii) why most of the Galactic GCs do not exhibit such internal abundance spreads. Our model demonstrates that the observed internal spreads of r -process elements in GCs provide strong evidence for prolonged star formation ($\sim 10^8$ yr).

Subject headings: globular cluster: general – galaxies: star clusters: general – galaxies: stellar content – stars:formation

1. INTRODUCTION

Recent photometric and spectroscopic investigation of the Galactic globular clusters (GCs) has confirmed that the GCs exhibit multiple stellar populations (see, e.g., Gratton et al. 2012 for a recent review). Individual GCs show internal abundance spreads in different elements: light elements (e.g., Carretta et al. 2009; C09), s -process (e.g., Marino et al. 2009), C+N+O (e.g., Yong et al. 2015), r -process (e.g., Snedin et al. 1997; Roederer 2011, R11; Sobeck et al. 2011, S11; Worley et al. 2013; W13), helium (e.g., Piotto et al. 2005), and Fe (e.g., Freeman & Rodgers 1975). Furthermore, the vast majority of the Galactic GCs investigated so far possess clear anti-correlations between light elements (e.g., CNO; C09). Such internal abundance spreads have also been observed for GCs in the Large and Small Magellanic Clouds (e.g., Mucciarelli et al. 2009; Niederhofer et al. 2016), and the Galactic dwarf satellites (e.g., Larsen et al. 2014). A key question related to GC formation is why GCs show both (i) ubiquitous anti-correlations between light elements (e.g., the Na-O anti-correlation) and (ii) a diversity in the degrees of chemical abundance inhomogeneity (e.g., only some GCs with [Fe/H] spreads).

Previous theoretical models of GC formation tried to reproduce the apparently universal anti-correlations between O and Na and between Mg and Al observed in the Galactic GCs (e.g., Fenner et al. 2004; Bekki et al. 2007; D’Ercole et al. 2008, 2010; Ventura et al. 2016). D’Antona, & Caloi (2004) discussed the origin of Y (helium abundance spread) in NGC 2808 based on the self-enrichment by mas-

sive AGB stars. The origin of GCs with abundance spreads in Fe and s -process elements has been recently discussed in the context of GC merging in their host dwarf galaxies (Bekki & Tsujimoto 2016). However, the origin of internal abundance spreads in r -process elements have not been discussed extensively so far, though not only M15 and M92 (e.g., Snedin et al. 1997; Roederer & Snedin 2011) but also several others (e.g., M5 and NGC 3201) are now observed to have such abundance spreads (e.g., R11). Tsujimoto & Shigeyama (2014, TS14) suggested that efficient accretion of r -process elements ejected from merging between neutron stars (neutron star merging; NSM) onto some fraction of (i.e., not all of) the stars in a GC can introduce a large star-to-star variation in the abundances of r -process elements within the GC.

If NSM ejecta can be mixed with an intra-cluster medium (ICM) and finally used for secondary star formation in a GC, then large star-to-star abundance spreads in r -process elements (e.g., [Eu/H]) can be expected. A key question here is whether the NSM ejecta with very high ejection speed (10 – 30% of the speed of light) can be stopped by the ICM within the forming GC ($R < 10$ pc). Recently Komiya & Shigeyama (2016) have shown that ejecta from NSMs can be stopped through interaction with the interstellar medium (ISM), because the ejecta can lose kinetic energy and momentum through interaction with the ISM. Recent numerical simulations have shown that a large amount of AGB ejecta can be accumulated in the central regions of forming GCs to form very high density gaseous regions with $\rho_g = 10^5$ cm⁻³ (Bekki

2017a, b, B17a,b). If a single NSM occurs in such a high-density gaseous region, then the ejecta is highly likely to be trapped and mixed with the AGB ejecta. New stars formed from such mixed gas can have chemical abundances of r -process elements that are quite different from those of stars formed in initial starburst at GC formation. Thus, it is possible that secondary star formation from AGB ejecta mixed with gas from a single NSM can explain the large internal abundance variations observed in several Galactic GCs (e.g., M5 and M15). This ‘NSM’ scenario has not been explored by previous theoretical works.

The purpose of this paper is to investigate the origin of GCs with internal abundance spreads in r -process elements based on the NSM scenario. We particularly investigate the following questions: (1) under what physical conditions NSM ejecta can be trapped within forming GCs, (2) what fraction of NSM ejecta can be trapped within GCs and used for secondary star formation, and (3) whether the degrees of internal abundance spreads depend on the physical properties of GCs (e.g., initial total masses). To do so, we use both analytical models and numerical simulations of GC formation from star-forming molecular clouds. We provide predictions of (i) the number of GCs with such internal abundance spreads (e.g., $\Delta[\text{Eu}/\text{H}]$), (ii) the bimodal distributions of $[\text{Eu}/\text{H}]$ in GCs, and (iii) possible correlations between $[\text{Na}/\text{Fe}]$ and $[\text{Eu}/\text{H}]$.

The plan of the paper is as follows. We discuss the possibility of NSM ejecta being trapped by the ICM of forming GCs using analytical models in §2. We derive the possible internal spreads of $[\text{Eu}/\text{H}]$ among GC stars by assuming secondary star formation from NSM ejecta mixed with the ICM in §3. We present the results of numerical simulations of GC formation to discuss whether the ICM of forming GCs can be as high as the required density of the ICM for trapping the NSM ejecta in §4. Based on these results, we provide several predictions of the NSM scenario in §5. We summarize our conclusions in §6. In order to discuss the present results, we show some observational results (W13) in Appendix A: the distribution of $[\text{Eu}/\text{H}]$ and a correlation between $[\text{Eu}/\text{H}]$ and $[\text{Na}/\text{Fe}]$ for M15.

2. THE SCENARIO

2.1. Ruling out supernovae as a source of r -process elements in GCs

There are two possible sites for the production of r -process elements, i.e., SNe and NSMs. Therefore, the following two possible scenarios for the origin of the internal chemical abundance spreads of r -process elements in GCs are promising. One is that the intra-cluster medium (ICM) of a GC-forming molecular cloud (MC) is chemically polluted by ejecta from several supernovae (SNe) so that new stars formed from the polluted gas can have $[\text{Eu}/\text{H}]$ different from those of stars formed from original gas (‘SN scenario’). The other is that new stars can be formed from gas ejected from NSMs much later than the initial burst of star formation in GCs (‘NSM scenario’). In the SN scenario, all stars with different $[\text{Eu}/\text{H}]$ should be formed before gas is completely expelled by SNe (i.e., $< 10^7$ yr), which means that GCs are simply a single generation of stars. Since the delay time (t_{delay}) distributions of NSMs has an extended distribution ($10^7 \leq t_{\text{delay}} \leq 10^{10}$ yr) with a peak around $t_{\text{delay}} = 3 \times 10^7$ yr (e.g., Dominik et al.

2012), secondary star formation in the NSM scenario can occur after all gas is removed from the GC-forming MC. This means that prolonged star formation is required in the NSM scenario.

We can rule out the SN scenario as follows. If SNe are the site of heavy r -process elements such as Ba and Eu, they inevitably produce both light (Y, Sr, etc) and heavy (Ba, Eu, etc) r -process elements. In M15, the stars which are enhanced in Ba and Eu abundances do not exhibit any enhancement in Sr. In other words, a large scatter is seen only in Ba and Eu while no spread in light r -process elements is found (e.g., S11). This observational result strongly suggests that SNe are not associated with the observed internal spreads in r -process elements of GCs (M15). Furthermore, the observed lack of metallicity spreads in GCs ($[\text{Fe}/\text{H}] < 0.05$ dex; C09) is inconsistent with the SN scenario, because if the ICM of forming GCs is polluted by r -process elements, then other elements (e.g, Mg and Fe) are also polluted to a large extent, ending up with rather large metallicity spreads. We thus rule out this SN scenario and accordingly discuss exclusively the NSM scenario in the present study.

2.2. Secondary star formation in mixed gas from AGB stars and NSMs

Figure 1 describes the new NSM scenario of GCs with internal abundance spreads in r -process elements (e.g., $[\text{Eu}/\text{H}]$). In the new scenario, the FG (first generation) stars are formed from a GC-forming molecular cloud. After all massive stars with the masses (m) larger than $9M_{\odot}$ exploded as SNe, gas ejected from AGB stars begins to be accumulated into the central region of the FG stellar system. The formation of SG (second generation) stars in the central high-density gaseous region is possible due to accretion of AGB ejecta. One NSM occurs during this accretion phase when the density of intra-cluster medium (ICM) in the central FG system becomes quite high ($\rho_{\text{icm}} > 10^4 M_{\odot}$). As a result of this, the ejecta from the NSM can be trapped by the ICM very efficiently, owing to interaction between the NSM ejecta and hydrogen atoms. New stars are then formed from the ICM mixed with the NSM ejecta, so that $[\text{Eu}/\text{H}]$ of the new stars can be much higher than those of FG stars. It should be stressed here that SG stars formed before the NSM can have almost identical $[\text{Eu}/\text{H}]$ as FG stars.

If the NSM occurs after the AGB ejecta are removed from a GC by some physical processes, such as expulsion of the gas by SNIa and ram pressure stripping of the gas by the Galactic hot halo gas or by the warm gas of the GC-host dwarf galaxy, then such a GC cannot show internal spreads in r -process elements. This is because there is no gas that can stop the r -process elements ejected from an NSM in the forming GC. Accordingly, the timing of an NSM within a forming GC is quite important as to whether the GC can finally have abundance spreads in r -process elements. Since neutron stars are the outcome of deaths of massive stars ($> 10M_{\odot}$ for which stars finally become SNe), NSMs occur only after SNe in forming GCs. Therefore, gas ejected from SNe should be all removed before the formation of SG stars. Otherwise, this scenario cannot explain the observed lack of abundance spreads in $[\text{Fe}/\text{H}]$ among GCs with internal spreads in r -process el-

ements. Given the wide range of delay-time distributions for NSMs (e.g., Dominik et al. 2012), it is possible that NSM events can occur more than 1 Gyr after the formation of FG stars in GCs. This could explain why only a fraction of old GCs shows significant abundance spreads in r -process elements (e.g., R11, W13).

In this scenario, FG and SG stars formed before NSMs should show smaller [Eu/H] than SG stars formed after NSMs. As discussed later in this paper, high [Eu/H] can be seen in SG stars with higher [Na/Fe] in M15, which is consistent with the new scenario. SG stars with very high [Na/Fe] formed from gas ejected by massive AGB stars ($m \sim [8 - 9]M_{\odot}$) might be less likely to have high [Eu/H], because the time interval between the onset of AGB phase for such intermediate-mass ($m \sim [8 - 9]M_{\odot}$) stars and the last (lowest mass) SNe is very short: fine-tuning is required for the epoch of an NSM. The wide spread of [Eu/H] in SG stars with different [Na/Fe] is expected in this scenario, if one NSM occurs when intermediate-mass stars ($[3 - 9]M_{\odot}$) enter into the AGB evolutionary stage.

A key question in this scenario is how much gas (ICM) is required to stop r -process elements ejected from NSMs, so that the NSM ejecta can be trapped in the central regions of GCs. Komiya & Shigeyama (2016) analytically investigated how r -process elements from an NSM can lose their initial kinetic energy through interaction with neutral hydrogen. They estimated how long the r -process elements can travel before they lose all of their kinetic energy through Coulomb scattering, and found that the ‘stopping length’ (l_s) is described as follows:

$$l_s = 2.6 \left(\frac{n_{\text{HI}}}{1 \text{ cm}^{-3}} \right)^{-1} \text{kpc}, \quad (1)$$

where n_{HI} is the number density of hydrogen atoms. This l_s should be as small as the core sizes of forming GCs ($\sim [2 - 3]$ pc) where secondary star formation should occur. It should be noted here that Tsujimoto et al. (2017) derived l_s using the observed abundances of ^{244}Pu of pre-solar grains, and pointed out that l_s can be significantly smaller than that derived by Komiya & Shigeyama (2016). Therefore, l_s in the above equation is an upper limit for l_s .

Figure 2 shows l_s as a function of the total mass of AGB ejecta (M_{gas}) for a given size of gas sphere (R_{gas}). Here the AGB ejecta is assumed to form a uniform gaseous sphere just for simplicity of discussion. Clearly, if $M_{\text{gas}} > 10^4 M_{\odot}$ and $R_{\text{gas}} < 3$ pc, then l_s can be smaller than 3 pc. This required M_{gas} is reasonable for GCs with initial total masses ($M_{\text{gc},0}$) of $\sim 10^5 M_{\odot}$, because $\sim 10\%$ of the masses in AGB stars can be ejected through stellar winds (e.g., Bekki 2011). If $M_{\text{gas}} \sim 10^{5.5} M_{\odot}$, then r -process elements can be trapped by the gas that is more diffusely distributed (i.e., $R_{\text{gas}} \sim 10$ pc). These results imply that retaining NSM ejecta in the central regions of forming GCs are highly likely after gas ejected from AGB stars is accumulated in the central regions.

If an NSM occurs within the gaseous sphere of a FG stellar system with a mass of $M_{\text{FG}} \geq 10^5 M_{\odot}$ and $R_{\text{gas}} < 3$ pc, then almost all of the NSM ejecta can be retained by the gas. If an NSM occurs outside the gaseous sphere of the FG stellar system, then only a fraction of the NSM ejecta can be trapped by the gas (i.e., AGB ejecta). Figure 3 shows the fraction of NSM ejecta retained by a GC (f_{ret}), as a function of the distance of the NSM from the center

of the GC (r_{gc}), for three $R_{\text{gas}} = 1, 3,$ and 10 pc. Since the flux of mass ejected from an NSM falls as r_{g}^{-2} , f_{ret} can be rather small outside R_{gas} . It is likely that only a fraction of NSM ejecta can be retained in GCs, because NSMs are likely to occur in the outer regions of GCs ($R > 3$ pc, where more stars can exist) than the central regions.

We can estimate (i) the [Eu/H] of stars formed from NSM ejecta mixed with AGB ejecta in a GC and (ii) internal abundance spreads of [Eu/H] among FG and SG stars ($\Delta[\text{Eu}/\text{H}]$) in the GC for a given f_{ret} by using the following simple model for mixing of AGB and NSM ejecta. We assume that the AGB and NSM ejecta can be mixed uniformly so that the final abundance of Eu depends on the total mass of AGB ejecta for a given yield of Eu from NSM events. The total mass of gas ejected from one NSM (M_{nsm}) is $\sim 0.01 M_{\odot}$ and the mass fraction of Eu in the ejecta ($f_{\text{Eu},0}$) is 10^{-2} (TS14). Using these numbers, we can calculate the chemical abundance of Eu (f_{Eu}) as follows:

$$f_{\text{Eu}} = \frac{f_{\text{Eu},0} M_{\text{nsm}} + f_{\text{Eu,agb}} M_{\text{gas}}}{M_{\text{agb}}}, \quad (2)$$

where M_{gas} is the total mass of AGB ejecta and $f_{\text{Eu},0}$ and $f_{\text{Eu,agb}}$ are the mass fractions of Eu in the NSM and AGB ejecta, respectively. We here ignore the total mass of NSM ejecta in the denominator, because it is too small in comparison with M_{gas} . We can convert this f_{Eu} into the final [Eu/H] of the mixed gas ($[\text{Eu}/\text{H}]_f$) by assuming the solar abundance of Eu (3.8×10^{-10}) for a given initial [Eu/H] ($[\text{Eu}/\text{H}]_i$) of AGB ejecta. The [Eu/H] spread is thus estimated as follows:

$$\Delta[\text{Eu}/\text{H}] = [\text{Eu}/\text{H}]_f - [\text{Eu}/\text{H}]_i. \quad (3)$$

Figure 4 shows $\Delta[\text{Eu}/\text{H}]$ for a metal-poor GC with $[\text{Eu}/\text{H}]_i = -2$ as a function of M_{gas} for three different f_{ret} . Clearly $\Delta[\text{Eu}/\text{H}]$ for this metal-poor GC can be quite large (≥ 1 dex) even for $f_{\text{ret}} = 0.01$, if $M_{\text{gas}} \leq 10^{4.4} M_{\odot}$. The GC with $M_{\text{gas}} \leq 10^5 M_{\odot}$ has $\Delta[\text{Eu}/\text{H}]$ much larger than the observed one for M15 (~ -1). A particular combination of M_{gas} and f_{ret} is required for the observed $\Delta[\text{Eu}/\text{H}]$ to be reproduced. Since GCs with $M_{\text{gc},0}$ can have $M_{\text{gas}} \sim 10^4 M_{\odot}$, these results suggest that only a small fraction of NSM ejecta should be mixed with ICM and retained in the GCs. If $M_{\text{gc},0}$ is significantly larger than $2 \times 10^5 M_{\odot}$ (typical present-day GC mass), then f_{ret} can be larger. These results combined with those in Figure 4 imply that GCs with internal abundance spreads of r -process elements experience only one NSM event in the outer part of the GCs in their early phases of formation. A future numerical study will investigate where NSM events can occur in forming GCs with AGB ejecta.

3. ANALYTICAL MODELS FOR [EU/H] SPREADS

Observational study of [Ba/H] distributions of GCs with internal [Ba/H] spreads showed a bimodal distribution of [Ba/H] in M15 (W13), and the [Eu/H] distribution in the data by W13 and S11 shows such a bimodality in the [Eu/H] distribution for M15 (see Appendix A). It is thus important to discuss whether and how the observed bimodality can be achieved in the present scenario of GC formation. Guided by recent results from hydrodynamical simulations of turbulent diffusion (Greif et al. 2009), we consider that r -process elements ejected from NSMs can be spread over the ICM of a forming GC through diffusion processes within a short timescale ($< 10^6$ yr). We adopt

a working hypothesis that the chemical abundances of Eu can be different in different regions of the ICM owing to turbulent diffusion. Although gaseous regions close to an NSM event can have very high [Eu/H] initially, the Eu abundances can become progressively lower as time passes owing to diffusion. We accordingly consider that the following functional form (the Green function) described in Greif et al. 2009) for the distribution of [Eu/H] for stars formed from NSM ejecta mixed with AGB ejecta:

$$N([\text{Eu}/\text{H}]) = \frac{N_0}{(2\pi\sigma^2)^{3/2}} \exp\left(\frac{-(Z - Z_m)^2}{2\sigma^2}\right), \quad (4)$$

where N_0 is the normalization constant, σ is the dispersion of [Eu/H], Z represents [Eu/H] (just for convenience), and Z_m is the mean value of [Eu/H].

These means and dispersions in [Eu/H] are different between the stars formed from original gas of a GC-forming MC (FG) and those from NSM ejecta mixed with AGB ejecta (SG). If SG stars are formed from AGB ejecta before NSMs occur, then [Eu/H] should be the same as those of FG stars. Accordingly, there could be a significant difference in [Eu/H] even in SG stars. Therefore, we use the two terms ‘polluted’ (‘p’) and ‘non-polluted’ (‘np’) to discriminate between stars that are formed from gas polluted by NSM ejecta and those without such pollution. For example, N_p and σ_p are the number of polluted stars and their [Eu/H] dispersion, respectively. A basic parameter for the entire distribution of [Eu/H] is σ_p , σ_{np} , Z_p , Z_{rp} , and R_p , which is the number ratio of polluted to non-polluted stars:

$$R_p = \frac{N_p}{N_{np}}. \quad (5)$$

Figure 5 shows the normalized N_p and N_{np} in the four models with different R_p , σ_p , and σ_{np} . For consistency with observations by W13, we adopt $Z_m = -2.0$ and -1.6 for non-polluted and polluted stars, respectively. Clearly, the [Eu/H] distributions depend strongly on the three parameters, with the model with R_p being the most similar to the observed distribution. The relatively large [Eu/H] dispersion (0.1 dex) in the best model with $R_p = 3.4$ implies that diffusion of r -process elements can proceed efficiently within the ICM of the GC. The present study cannot discuss whether such a large dispersion of 0.1 dex can be achieved in the ICM though turbulent diffusion. The larger R_p implies that 77% of the present stars in M15 can be the polluted population. The large fraction of the polluted population in M15 implies that the original mass of FG (non-polluted) stars, from which AGB ejecta originates, should be at least by a factor of ~ 10 larger than the present-day mass of the FG - This is a classic mass-budget problem discussed by many previous works (e.g., Smith & Norris 1982). The selective stripping of FG stars in the early phase of GC formation is a promising explanation for solving this mass budget problem (Bekki 2011).

4. NUMERICAL SIMULATIONS OF GAS ACCUMULATION FROM AGB STARS

In order to discuss whether the density of ICM of forming GCs can become as high as $\rho_{\text{icm}} = 10^4 \text{ cm}^{-3}$, we perform smooth particle hydrodynamics (SPH) simulations of

GC formation within massive MCs. We have already investigated the general trends of GC formation within MCs (B17b), and we use the same numerical methods used in B17b in the present study. Since the details of the numerical methods are given in B17b, we briefly describe them in this paper. We use our original simulation code that can be run on a cluster of GPU (Graphics Processing Unit) machines (Bekki 2013, 2015). A MC with a total mass of M_{mc} and a size of M_{mc} is assumed to have (i) a fractal mass distribution with the three-dimensional fractal dimension of 2.6 and (ii) a power-law radial density distribution with a slope of -1 . The initial virial ratio of a GC-forming MC is set to be 0.35, which ensures rapid gravitational collapse of the MC. The initial global rotation of fractal MCs is not included in the present study.

Feedback effects of SNe with different masses are separately implemented in the simulations, and the gas ejection of individual AGB stars is also self-consistently included. Star formation is assumed to occur (i) if the gas density of a particle (ρ_g) exceeds the threshold gas density of star formation (ρ_{th}) and (ii) if $\text{div}v < 0$, where v is the velocity of the gas particle. We adopt $\rho_{\text{th}} = 10^5 \text{ cm}^{-3}$ in the present study. We consider the following two models for star formation from AGB ejecta. In one model (M1), star formation cannot occur from AGB ejecta even if $\rho_g \geq 10^5 \text{ cm}^{-3}$. This model is constructed to obtain the better understanding of the density enhancement achieved through accumulation of AGB ejecta in the central regions of forming GCs. In the other model (M2), star formation occurs if the above two physical conditions are met for AGB ejecta.

We here describe the results of the models (M1 and M2) with $M_{\text{mc}} = 3 \times 10^6 M_\odot$ and $R_{\text{mc}} = 100 \text{ pc}$ for which GCs with the final stellar mass (M_{gc}) being $\sim 10^6 M_\odot$ can be formed. The mass and spatial resolutions of the models are $2.9 M_\odot$ and 0.2 pc in the present study. The total number (N) of a simulation significantly increases from the initial $N = 1048911$ owing to the new addition of ‘AGB particles’ which represent gas ejected from AGB stars with different masses.

Figures 6, 7, and 8 describe how the AGB ejecta can be accreted into the central region of a forming GC within a giant MC in the fiducial model M1 without secondary star formation from AGB ejecta. FG stars are formed from numerous small gas clumps that are developed from local gravitational instabilities within the fractal MC, because ρ_g of the small clump can become higher than 10^5 cm^{-3} . These numerous groups of FG stars merger with one another to form a larger stellar system with a stellar halo within a timescale of 10^7 yr (at $T = 12 \text{ Myr}$). The gas density of the GC-forming MC can dramatically decrease owing to gas consumption by the FG formation. The remaining cold gas of the MC can be rapidly expelled by multiple SN explosion ($T = 12$ and 24 Myr) because the lifetimes of massive stars with $m > 30 M_\odot$ is quite short ($< 10 \text{ Myr}$). The cold gas gradually disappears from the inner region of the forming GC ($T = 36 \text{ Myr}$), and almost all of the gas can be expelled from the GC by $T = 110 \text{ Myr}$.

Massive AGB stars ($m = [6 - 9] M_\odot$) start to eject (Na-rich) gas after the removal of gas chemically polluted by SN explosion ($T \sim 50 \text{ Myr}$). The AGB ejecta can be gravitationally trapped in the FG stellar system with a total

mass of $\sim 2 \times 10^6 M_\odot$ because of the relatively slow wind velocity ($v_{\text{wind}} = 10 \text{ km s}^{-1}$). The gas can be gradually accumulated onto the central regions ($R < 2 \text{ pc}$) of the FG stellar system ($T = 110 \text{ Myr}$), so that ρ_g can become very high. The gas can efficiently lose its kinetic energy owing to energy dissipation of the gas during its accretion process within the GC. Finally a very compact gaseous sphere in the central region of the FG stellar system can be formed 149 Myr after the start of gravitational collapse of the MC in this model. These basic formation processes of a GC can be seen in the model M2 with secondary star formation from AGB ejecta.

Figure 9 shows the radial distributions of ρ_{icm} at $T = 149 \text{ Myr}$ for M1 and M2. Since star formation is not included in M2, ρ_{icm} can become rather high $> 10^5 \text{ cm}^{-3}$ in the center of the FG stellar system ($R < 0.4 \text{ pc}$). Clearly, most of the gas particles within $R < 1 \text{ pc}$ has $\log \rho_{\text{icm}} \geq 3.4$ that is required for $l_s \leq 3 \text{ pc}$ (for stopping of r -process elements and trapping them within GCs). This means that if NSMs occur around this time step ($T = 149 \text{ Myr}$), then the ejecta can be easily trapped by the ICM in this model. It is confirmed that ρ_{icm} can be also quite high ($\rho_{\text{icm}} > 10^4 \text{ cm}^{-3}$) at $T = 110 \text{ Myr}$, which means that fine-tuning in the epoch of an NSM is not required for the ejecta to be trapped by the ICM.

However, secondary star formation from AGB ejecta can continue to decrease the total mass of the ICM so that ρ_{icm} can be significantly lower. Figure 9 shows that although the radial gradient of ρ_{icm} is very steep, ρ_{icm} in the inner region of the simulated GC can still be high ($> 10^4 \text{ cm}^{-3}$) in M2 with secondary star formation. This confirms that as long as ρ_{th} is similar to the gas densities of the molecular cores of star-forming MCs (10^5 cm^{-3}), then AGB ejecta (ICM) can continue to have $\rho_{\text{icm}} \geq 10^4 \text{ cm}^{-3}$ over several Myrs. We thus conclude that AGB ejecta can stop the r -process elements ejected from an NSM so that the NSM ejecta can be used for secondary star formation in the central region of a forming GC.

5. DISCUSSION

5.1. The epoch of an NSM in a forming M15

Recent spectroscopic studies of chemical abundances of stars have investigated some correlations between light (Na and O) and r -process elements (Ba and Eu) for M15 (W13 and S11). Appendix A describes the results of our own investigation of the correlations using the same data sets. Clearly, no stars are located in the area with $[\text{Na}/\text{Fe}] > 1.0$ and $[\text{Eu}/\text{H}] > -1.8$ in M15 whereas there is a strong concentration of Eu-rich stars around $[\text{Na}/\text{Fe}] \sim 0.3 - 0.6$. The absence of stars with high $[\text{Na}/\text{Fe}]$ and high $[\text{Eu}/\text{H}]$ might have some physical meaning for the formation of M15. Since an NSM can occur anytime during GC formation, it is possible that only SG stars formed after the NSM can have large $[\text{Eu}/\text{H}]$.

Ventura et al. (2011) predicted that gas ejected from (i) massive AGB stars with $m = 8M_\odot$ (and shorter lifetimes) can have $[\text{Na}/\text{Fe}] \sim 1.0$, whereas those with $m \leq 7.5M_\odot$ have lower $[\text{Na}/\text{Fe}]$ (longer lifetimes). Therefore, if an NSM occurs well after gas ejected from AGB stars with $m = 8M_\odot$ is consumed by secondary star formation, then the absence of such Na-rich and Eu-rich stars is expected. This means that an NSM should have occurred at least

$3 \times 10^7 \text{ yr}$ (i.e., lifetime of the lowest mass SN) after the initial burst of star formation in M15. It is possible that the concentration of $[\text{Eu}/\text{H}]$ around $[\text{Na}/\text{Fe}] \sim [0.3 - 0.5]$ indicates the epoch of an NSM in the early formation phase of M15. It is observationally unclear whether such an absence of stars with high $[\text{Na}/\text{Fe}]$ and high $[\text{Eu}/\text{H}]$ can be seen in other GCs with internal spreads of r -process elements. Therefore, we cannot make a robust conclusion on whether the distribution of stars on the $[\text{Na}/\text{Fe}]$ - $[\text{Eu}/\text{H}]$ diagram for a GC has fossil information on the epoch of a NSM in the GC.

5.2. Why do only several GCs show abundance spreads in r -process elements

R11 investigated the chemical abundances of r -process elements for 17 Galactic GCs, and found that only 4 GCs among them have large internal spreads of $[\text{Eu}/\text{H}]$. So far only these GCs are those with clear evidence of internal abundance spreads in r -process elements among all Galactic GCs. This observation raised a question as to why only a fraction of GCs show such clear abundance spreads of $[\text{Eu}/\text{H}]$ in the Galaxy. In the present NSM scenario, NSMs need to occur when forming GCs still retain an enough amount of AGB ejecta ($> 10^3 M_\odot$). Forming GCs can lose their AGB ejecta by some physical processes such as (i) ram pressure stripping by warm/hot gas of their GC-hosting galaxies and (ii) prompt type Ia SNe. Accordingly, NSMs need to occur before stripping of AGB ejecta for the ejecta to be converted into new stars. Given the observed wide range of the delay time (t_{delay}) distribution of NSMs ($[10^7 - 10^{10}] \text{ yr}$), NSMs do not so easily synchronize with when GCs still retain AGB ejecta. Therefore, only GCs that happened to experience NSMs during secondary star formation from AGB ejecta can have internal abundance spreads in r -process elements.

We discuss the probability (P_r) of one GC to have one NSM in a more quantitative way as follows. The t_{delay} distribution of NSMs has the following power-law profile for $t_{\text{delay}} > 3 \times 10^7 \text{ yr}$ (Figure 8 in Dominik et al. 2012):

$$\frac{dN}{dt} \propto t_{\text{delay}}^{-\beta}, \quad (6)$$

where β can be approximated as 1.3. If the duration of secondary star formation from AGB ejecta is t_{sf} , then P_r is described as follows:

$$P_r = \frac{n_{\text{nsm}} t_{\text{sf}}}{t_{\text{delay},m}}, \quad (7)$$

where n_{nsm} is the number of NSMs that can occur in one GC and $t_{\text{delay},m}$ is the average of t_{delay} . The total number of GCs with internal abundance spreads in r -process elements in the Galaxy ($N_{\text{gc},r}$) is as follows:

$$N_{\text{gc},r} = P_r N_{\text{gc},0}, \quad (8)$$

where $N_{\text{gc},0}$ is the number of the Galactic GCs. The total number of core collapse SNe (CCSNe) that occur in one GC (with a total mass of $\approx 10^5 M_\odot$) is ≈ 500 , and one NSM occurs for every 1500 CCSNe (Tsujimoto et al. 2017). Therefore, $n_{\text{nsm}} = 500/1500 = 0.3$ is a reasonable value. If we adopt reasonable numbers for $t_{\text{delay},m}$ ($= 10^9 \text{ yr}$; Dominik et al. 2012) and $t_{\text{sf}} = 10^8 \text{ yr}$ and $n_{\text{nsm}} = 0.3$, then $N_{\text{gc},r} = 4.5$ for $N_{\text{gc},0} = 150$ (Harris 1996 - 2010 edition). This is roughly consistent with the number of GCs with internal abundance spreads in r -process elements.

5.3. Alternative scenarios

We have so far assumed that multiple generations of stars formed from NSM ejecta (which are diluted by AGB ejecta) are responsible for the origin of GCs with internal abundance spreads in r -process elements. There are the following two alternative scenarios for the origin. One is the ‘gas accretion’ scenario in which only a fraction of GC stars can accrete NSM ejecta, so that they can show enhanced $[\text{Eu}/\text{H}]$. The other is a ‘merging scenario’ in which two GCs with different $[\text{Eu}/\text{H}]$ merge with each other to form a new GC with a $[\text{Eu}/\text{H}]$ spread. In the gas accretion scenario, all GC stars were born almost simultaneously within in a GC-forming MC, and only some fraction of the stars can significantly change their chemical abundances through accretion of NSM ejecta into the GCs. Gas accretion occurs for the stars in the core of a GC, whereas stars outside the core are not affected by gas accretion in this scenario. Therefore, there should naturally be the bimodality in the $[\text{Eu}/\text{H}]$ distribution, as claimed by TS14. In order for NSM ejecta to be retained in forming GCs, a high-density ICM ($\rho_{\text{icm}} > 10^6 M_{\odot}$) is required (TS14). Although this can be achieved, as shown in M1 of the present study, a serious problem remains for this scenario. The observed dispersion of $[\text{Na}/\text{Fe}]$ for a given $[\text{Eu}/\text{H}]$ would be difficult to explain, because the gas accretion process does not depend on whether the gas comprises NSM or AGB ejecta.

In the merger scenario, two GCs with similar masses and $[\text{Fe}/\text{H}]$ yet quite different $[\text{Eu}/\text{H}]$ need to merge with each other. Even if GC merging is possible in dwarf galaxies, as demonstrated by recent numerical simulations of GC merging (Bekki & Yong 2012; Bekki & Tsujimoto 2016), this scenario has the following problems. First, it is unclear why the merging two GCs had almost identical metallicities yet different $[\text{Eu}/\text{H}]$ at the time of merging, if the merging is between two GCs that were possibly formed in different parts of the host dwarf galaxy. Secondly, the merging scenario cannot simply explain why more Na-rich stars are more likely to have high $[\text{Eu}/\text{H}]$ for $[\text{Na}/\text{Fe}] < 1$ in M15. Thus, the present NSM merger scenario appears to be more promising than the other two, though it still must resolve the mass budget problem.

5.4. Relation to the Galactic halo stars

The Galactic stellar halo contains very metal-poor stars ($[\text{Fe}/\text{H}] < -2$) with highly enhanced abundances of r -process elements (e.g., Beers & Christlieb 2005). It remains unclear where these ‘r-I’ ($0.3 \leq [\text{Eu}/\text{Fe}] \leq 1$ and $[\text{Ba}/\text{Fe}] < 0$) and ‘r-II’ ($1 < [\text{Eu}/\text{Fe}]$ and $[\text{Ba}/\text{Fe}] < 0$) stars originate. At least some of them could have been initially in GCs with large $[\text{Eu}/\text{H}]$ spreads like M15, and stripped from the GCs at later times. In addition, it is possible that they were initially in the building blocks of the Galaxy, i.e., defunct dwarf galaxies. Recently, Ji et al. (2016) have discovered the presence of stars with high $[\text{Eu}/\text{H}]$ and $[\text{Ba}/\text{H}]$ in an ultra-faint dwarf galaxy (UFD), Reticulum II (Ret II), which are identical to r-II stars in the Galactic halo. Thus, it suggests that r-II stars could also be from UFDs. It would be an important question how we can distinguish between r-II stars from GCs, UFDs, and other types of defunct dwarf galaxies.

Our NSM scenario predicts that some of r-II stars in

forming GCs can have high Na abundances. In fact, most of r-II stars exhibit $[\text{Na}/\text{Fe}] \approx 0.5-1$ (Suda et al. 2008), which is compatible with their origin associated with GCs like M15. The above discussion can be used to classify the origin of individual r-II stars into UFDs or GCs, because r-II stars from UFDs cannot have such highly enhanced Na abundances. On the other hand, given the lowest metallicity of -2.5 for the Galactic GCs (e.g., Harris 1991), the r-II stars with $[\text{Fe}/\text{H}] < -2.5$ in the Galactic halo are unlikely to be from GCs, whereas the r-II stars in Ret II cover the metallicity range of $-3 < [\text{Fe}/\text{H}] < -2$ (Ji et al. 2016). In addition, there are two factors which reduce the contribution to field r-II stars from GCs. First, more massive GCs are less likely to lose their stars owing to tidal stripping of the stars during the orbital evolution of GCs around the Galaxy (e.g., Rossi et al. 2016). Secondly, stars enriched with r -process elements are predicted to be formed in the central regions of forming GCs. Future large samples of r-II stars in the halo, when combined with information on both their metallicity distribution and elemental abundances, can reveal the entire picture of r-II stars assembling from GCs, UFDs, or other types of dwarf galaxies. It should be noted that carbon-enhanced metal-poor stars with large abundances of r -process elements (CEMP-r) cannot simply arise from GCs in the present NSM scenario, because the SG stars in GCs have highly enhanced N and depleted C, reflecting the abundances of massive AGB ejecta (e.g., Bekki et al. 2007).

The origin of r-II stars in Ret II could be related to efficient mixing of interstellar medium (ISM) and NSM ejecta, and subsequent star formation from the mixed gas in the early gas-rich phase, because all stars with $[\text{Fe}/\text{H}] > -3$ are highly enriched with r -process elements. If an NSM is assumed to occur within the ISM with $n_{\text{HI}} = 100$, then the NSM ejecta can be trapped within the central ~ 30 pc of the UFD, followed by star formation from this mixed gas. If we adopt a shorter l_s (stopping length for NSM ejecta) derived by Tsujimoto et al. (2017), then l_s becomes ~ 4 pc for $n_{\text{HI}} = 100$. In this case, subsequent star formation is considered to occur after the NSM ejecta spread throughout the ISM due to turbulent diffusion. From the observed $[\text{Eu}/\text{H}]$ spread in Ret II, we can deduce the ISM mass (M_{ISM}) mixed with NSM ejecta. Assuming a Eu mass from a single NSM, we obtain a large amount of gas of $M_{\text{ISM}} \sim 10^6 M_{\odot}$ (see also the discussion of Ji et al. 2016). On the other hand, Ret II is known to have the γ -ray signal likely induced by dark matter annihilation (e.g., Geringer-Sameth et al. 2015), which leads to the possibility of the high central density of dark matter in Ret II. Therefore, it is feasible to consider that the required high ISM density in the central few pc can be realized in the early gas-rich Ret II with a high dark matter density.

6. CONCLUSIONS

In order to understand the origin of GCs with internal abundance spreads in r -process elements (e.g., $[\text{Eu}/\text{H}]$), we have investigated whether ejecta from NSMs can be retained in forming GCs and subsequently converted into new stars using analytical models and numerical simulations of GC formation. In the present ‘NSM scenario’, stars with high $[\text{Eu}/\text{H}]$ are formed from NSM ejecta mixed with ICM (i.e., AGB ejecta) several tens of Myr after the

initial starburst of GC formation. Therefore, prolonged star formation is essential in this GC formation scenario. We have also constructed a theoretical model that explains the observed bimodal distribution of [Eu/H] in GCs. The principal results are as follows:

(1) The high-speed gaseous ejecta (i.e., r -process elements) from NSMs can be stopped by the ICM in forming GCs, if the total mass of the ICM within the central regions of GCs ($R \sim [1 - 3]$ pc) is as large as $10^4 M_\odot$. This means that AGB ejecta in GCs with the original stellar masses (M_s) of $\sim 10^5 M_\odot$ can stop the r -process elements from NSMs, because $\sim 10\%$ of M_s can be AGB ejecta. It is concluded that AGB ejecta is essentially important for trapping the NSM ejecta in the central regions of GCs. The required larger amount of AGB ejecta implies that the original GCs should be massive.

(2) NSMs can possibly occur more likely outside the central region of a GC than within the central region. Therefore, only the fraction of NSM ejecta can interact with the ICM (i.e., AGB ejecta), so that the mass fraction of the ejecta trapped and retained by the ICM (f_{ret}) can be very small (< 0.1). Our models suggest that small f_{ret} (~ 0.01) is required for explaining the observed spreads of [Eu/H] (e.g., $\Delta[\text{Eu}/\text{H}] \sim -1$ dex for M15). Therefore, one NSM in the outer part of a forming GC is not a problem in the present scenario.

(3) The observed apparent bimodal distribution of [Eu/H] in M15 can be explained if SG (second generation) stars were formed from ICM with the mean [Eu/H] being by ~ 1 dex higher than the initial [Eu/H] of the GC-forming MC. The observed large spread in [Eu/H] in the SG stars is due to turbulent diffusion of NSM ejecta in the ICM. The larger number of SG stars with enhanced [Eu/H] suggests that the original mass of the GC (M15) should be significantly larger than the present mass of the GC: this is the classic mass-budget problem in GC formation.

(4) Our new hydrodynamical simulations of GC formation from fractal MCs show that the required higher ICM density ($\rho_{\text{icm}} > [10^3 - 10^4] \text{ cm}^{-3}$) is possible ~ 100 Myr after the initial burst of stars formation in GCs. This result thus confirms the validity of the present NSM scenario. Although secondary star formation can decrease ρ_{icm} , the ICM can keep its higher density owing to slow

star formation in SG formation. We thus conclude that the NSM scenario is very promising in explaining the observed internal spreads of r -process elements in GCs.

(5) The scenario predicts that the number of GCs with such internal spreads of r -process elements should be small (≤ 5) owing to (i) the rarity of NSMs and (ii) the very wide distribution of delay time of NSMs. The scenario also predicts that there are two SG populations with low and high [Eu/Fe], which appears to be consistent with the observed [Eu/H]-[Na/Fe] relation for M15. Although the observed large number of stars with high [Eu/H] and high [Na/Fe] in M15 supports the NSM scenario, other GCs need to be investigated to make a more robust conclusion on the validity of the scenario.

(6) We rule out the possibility of unusual SNe (e.g., magneto-rotational SNe; Nishimura et al. 2017), as the origin of internal spreads of r -process elements in M15 for the following two reasons. First, if the ICM of forming GCs is chemically polluted by SNe, then internal abundance spreads can be seen not only in [Eu/H] but also in [Fe/H], which is not seen in GCs. Secondly, if SNe are the site of r -process elements, they produce both light (Y, Sr, etc) and heavy (Ba, Eu, etc) r -process elements. Stars with enhanced Ba and Eu, however, do not exhibit any enhancement in Sr or so in GCs (e.g., M15). The observed large scatter seen only in Ba and Eu (but not in light r -process elements) is inconsistent with the above (unusual) SN scenario.

(7) Since short gamma-ray bursts (GRBs) originate from NSMs (e.g., Grindlay et al. 2006), direct evidence for the NSM scenario would be the discovery of short GRBs located in very young and massive GCs with ages of $[10^7 - 10^8]$ yr at high redshifts. Such young GCs can also have very low-level star formation, and the optical light curves of the GRBs could be significantly influenced by dust (AGB ejecta) within the GCs. Although young, massive GCs with short GRBs shrouded by dust would be very hard to identify with current telescopes, owing to the low luminosities, the discovery of such GCs would provide irrefutable supporting evidence for the NSM scenario.

We are grateful to the referee, Timothy C. Beers, for his constructive and useful comments. TT is supported in part by JSPS KAKENHI Grant Number 15K05033.

REFERENCES

- Beers, T. C., Christlieb, N., 2005, *ARA&A*, 43, 531
 Bekki, K., 2011, *MNRAS*, 412, 2241
 Bekki, K., 2013, 432, 2298
 Bekki, K. 2015, *MNRAS*, 449, 1625,
 Bekki, K., 2017a, *MNRAS*, 467, 1857 (B17a)
 Bekki, K., 2017b, *MNRAS* in press, arXiv:1705.10039 (B17b)
 Bekki, K., Campbell, S. W., Lattanzio, J. C., Norris, J. E., 2007, *MNRAS*, 377, 335
 Bekki, K., Yong, D., 2012, *MNRAS*, 419, 2063
 Bekki, K., Tsujimoto, T., 2016, *ApJ*, 831, 70
 Carretta, E., Bragaglia, A., Gratton, R. G., Lucatello, S., 2009, *A&A*, 505, 117 (C09)
 D'Antona, F., & Caloi, V. 2004, *ApJ*, 611, 871
 D'Ercole, A., Vesperini, E., D'Antona, F., McMillan, S. L. W., & Recchi, S. 2008, *MNRAS*, 391, 825 (D08)
 D'Ercole, A., D'Antona, F., Ventura, P., Vesperini, E., McMillan, S. L. W., 2010, *MNRAS*, 407, 854 (D10)
 Dominik et al. 2012, *ApJ*, 759, 52
 Fenner, Y., Campbell, S., Karakas, A. I., Lattanzio, J. C., Gibson, B. K., 2004, *MNRAS*, 353, 789
 Freeman, K., & Rodgers, A. W., 1975, *ApJ*, 201, 71
 Geringer-Sameth, A., et al. 2015, *PhRvL*, 115, 1101
 Gratton, Raffaele G.; Carretta, Eugenio; Bragaglia, A., 2012, *A&ARv*, 20, 50
 Greif, T. H., Johnson, J. L., Klessen, R. S., & Bromm, V. 2009, *MNRAS*, 399, 639
 Grindlay, J., Portegies Zwart, S., & McMillan, S. 2006, *NatPh*, 2, 116
 Harris, W. E., 1991, *ARA&A*, 29, 543
 Harris, W.E. 1996, *AJ*, 112, 1487

- Ji, A. P., Frebel, A., Chiti, A., Simon, J. D. 2016, *Nature*, 531, 610
Komiya, Y., & ShigeYama, T. 2016, *ApJ*, 830, 76
Larsen, S. S., Brodie, J. P., Grundahl, F., Strader, J., 2014, *ApJ*, 797, 15
Larson, R. B., 1981, *MNRAS*, 194, 809
Marino, A. F., Milone, A. P., Piotto, G., Villanova, S., Bedin, L. R., Bellini, A., Renzini, A., 2009, *A&A*, 505, 1099
Mucciarelli, A., Origlia, L., Ferraro, F. R., Pancino, E., 2009, *ApJ*, 695, L134
Niederhofer, F., et al., 2016, *MNRAS* in press (arXiv:1612.00400)
Nishimura, N., Sawai, H., Takiwaki, T., Yamada, S., & Thielemann, F.-K., 2017, *ApJ*, 836, L21
Piotto, G., et al., 2005, 621, 777
Roederer, I. U., 2011, *ApJ*, 732, L17 (R11)
Rossi, L. J., Bekki, K., & Hurley, J. R., 2016, *MNRAS*, 462, 2861
Smith, G. H., & Norris, J., 1982, *ApJ*, 254, 594
Snedden, C., Kraft, R. P., Shetrone, M. D., Smith, G. H., Langer, G. E., & Prosser, C. F. 1997, *AJ*, 114, 1964
Sobeck et al. 2011, *AJ*, 141, 175 (S11)
Suda, T., et al. 2008, *PASJ*, 60, 1159
Tsujiimoto, T., & ShigeYama, T. 2014, *ApJ*, 795, L18 (TS14)
Tsujiimoto, T., Yokoyama, T., & Bekki, K. 2017, *ApJ*, 835, L3
Ventura, P., Carini, R., D'Antona, F., 2011, *MNRAS*, 415, 3865
Ventura, P., et al. 2016, *ApJ*, 831, L17
Vesperini, E., McMillan, S. L. W., D'Antona, F., & D'Ercole, A. 2010, *ApJ*, 718, L112
Worley, C. C., Hill, V., Sobeck, J., & Carretta, E. 2013, *A&A*, 553, 47 (W13)
Yong, D. Grundahl, F., & Norris, J. E. 2015, *MNRAS*, 446, 3319

APPENDIX

THE OBSERVED BIMODAL DISTRIBUTION OF $[\text{Eu}/\text{H}]$ AND CORRELATION BETWEEN $[\text{Na}/\text{Fe}]$ AND $[\text{Eu}/\text{H}]$ IN M15

Recent observational study of the Galactic GC M15 has revealed that the distributions of $[\text{Eu}/\text{H}]$ and $[\text{Ba}/\text{H}]$ (r -process elements) are bimodal with two distinct peaks (W13). We have reproduced the bimodal $[\text{Eu}/\text{H}]$ distribution using the data by W13 in order to discuss the present results of our theoretical models. Figure A1 shows that the $[\text{Eu}/\text{H}]$ distribution has two peaks around $[\text{Eu}/\text{H}] \sim -1$ and -1.6 , with a large dispersion for the entire population ($-2.2 \leq [\text{Eu}/\text{H}] \leq -1.2$; $\Delta[\text{Eu}/\text{H}] \sim 1.0$ dex). If one star with very Eu-rich abundance around $[\text{Eu}/\text{H}] \sim -1.2$ is removed, then the dispersion is 0.8 dex. The two peaks strongly suggest that there were two major episodes of star formation in M15. The physical origin for the two major episodes of star formation is given in the main text.

Using the same data for M15, we have investigated the distribution of stars in the $[\text{Na}/\text{Fe}]$ - $[\text{Eu}/\text{H}]$ diagram for M15. Figure A2 shows the following three trends for the GC stars. First, most of the stars with $0.3 \leq [\text{Na}/\text{Fe}] \leq 1.0$ (corresponding to SG stars) have higher $[\text{Eu}/\text{H}]$ (> -1.8 , i.e., around the second peak of the $[\text{Eu}/\text{H}]$ -distribution). Secondly, four stars with very high $[\text{Na}/\text{Fe}]$ (> 1.0) do not show such high $[\text{Eu}/\text{H}]$ (> -1.8). Thirdly, most of stars with $[\text{Na}/\text{Fe}] < 0$ have lower $[\text{Eu}/\text{H}]$ (< -1.8): it should be noted that one star with $[\text{Na}/\text{Fe}] \sim -0.1$ has a high $[\text{Eu}/\text{H}]$ (~ -1.5). The absence of stars with very high $[\text{Na}/\text{Fe}]$ and very high $[\text{Eu}/\text{H}]$ appears to be remarkable, though the number of stars investigated is not so large. Gas ejected from metal-poor, massive AGB stars with $m = 8M_{\odot}$ can have $[\text{Na}/\text{Fe}] \sim 1.0$ (e.g., Ventura et al. 2011). Therefore, one possible interpretation for the absence of such high-Na and high-Eu stars is that one NSM occurred after massive AGB stars died away. More details on this discussion is given in the main text.

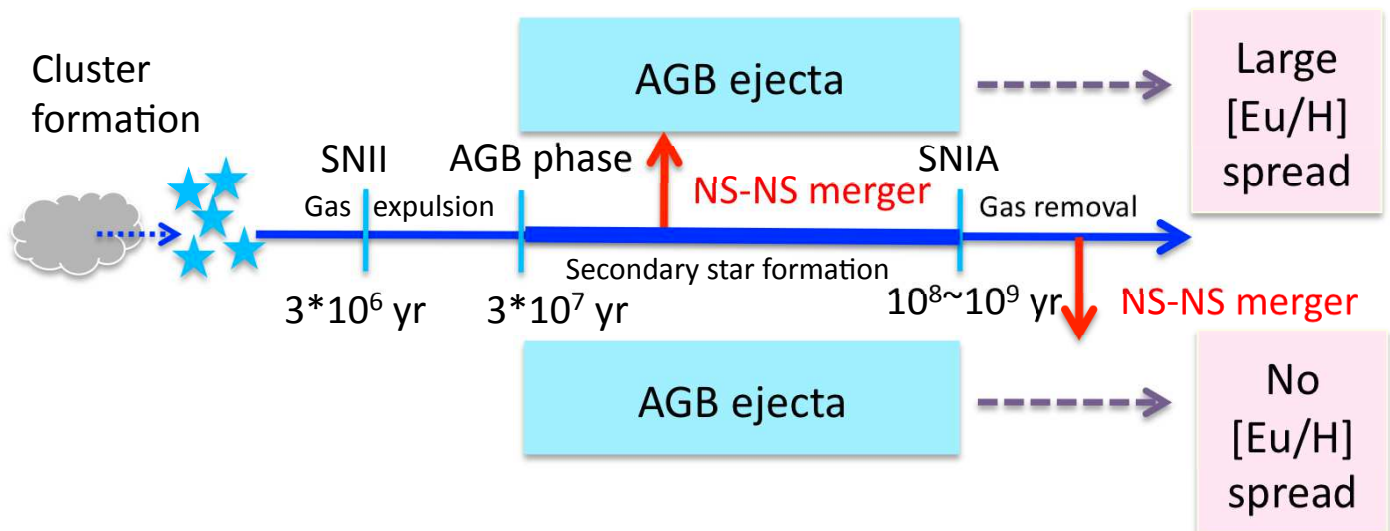


FIG. 1.— A schematic illustration of the new ‘NSM’ scenario of GC formation. In this scenario, FG (first generation) stars are formed from cold gas of a molecular cloud (MC). After all of the remaining gas left after FG formation is expelled by Type II SNe of FG ($T = [3 - 30] \times 10^6$ yr), gas ejected from AGB stars in FG stars to be accumulated into the central region of the forming GC around $T = 3 \times 10^7$ yr. SG (second generation) stars can be formed from the gas when the density of the intra-cluster medium (ICM) becomes as high as 10^5 cm^{-3} . A merger between neutron stars (‘NS-NS’ merger; ‘NSM’) occurs during this SG formation, and subsequently the NSM ejecta can mix with the ICM (i.e., AGB ejecta). The mixed gas is converted into new stars with chemical abundances of r -process elements significantly different from those of FG stars and those of SG stars formed before the NSM. All of the remaining ICM is removed from the forming GC owing to some physical processes, such as Type Ia SNe or ram pressure stripping by the GC-host galaxy. In this scenario, it depends on the epoch of an NSM in a forming GC whether the GC can finally have internal abundance spreads in r -process elements. If an NSM occurs in a GC after all of the gas is removed from the GC, then the GC cannot have such internal abundance spreads.

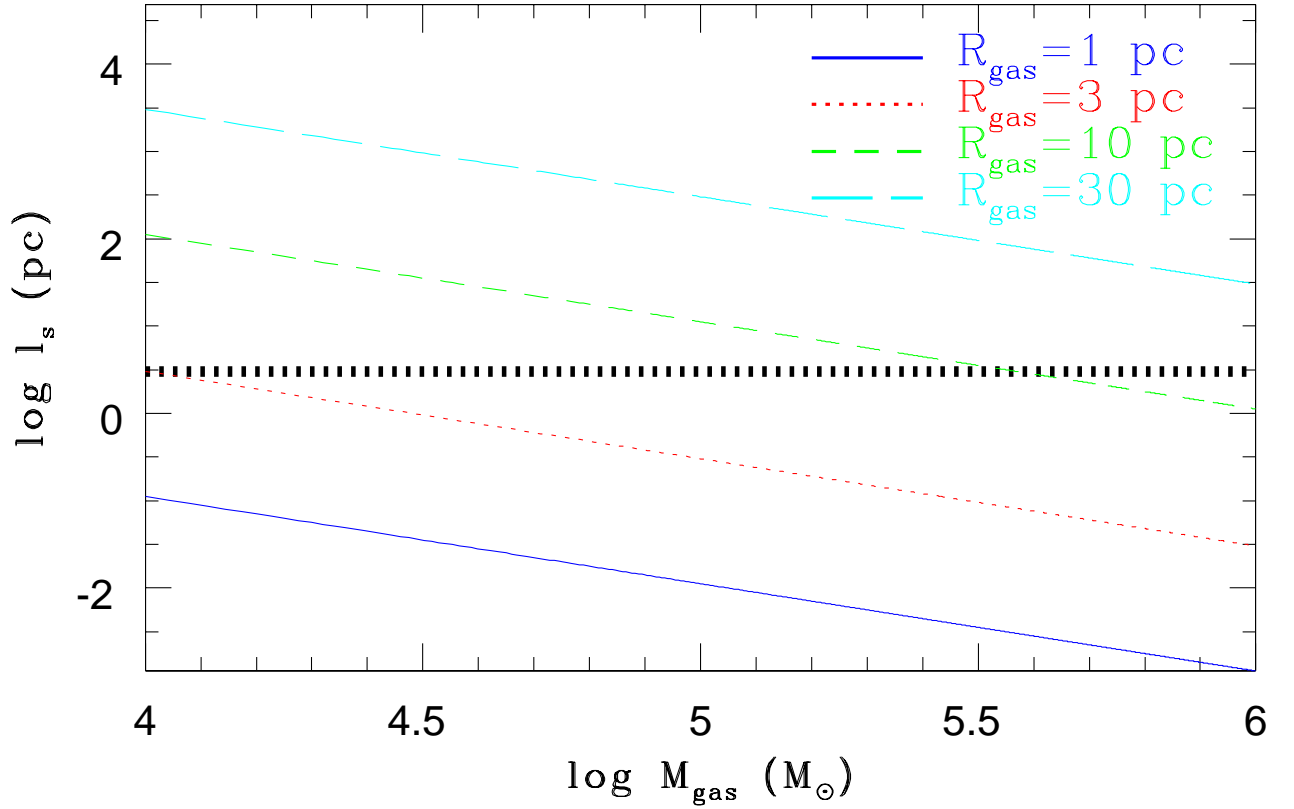


FIG. 2.— Stopping length (l_s) as a function of the total mass of gas (AGB ejecta) in a forming GC (M_{gas}) for $R_{\text{gas}}=1$ pc (blue solid), 3 pc (red dotted), 10 pc (green short-dashed), and 30 pc (cyan long-dashed), where R_{gas} is the radius of the gaseous sphere formed from the AGB ejecta. If $l_s = 1$ pc, then it means that a r -process element can be stopped through interaction with gas (mainly neutral hydrogen) after it freely moves for 1 pc. The thick black dotted lines indicates the point where l_s becomes the typical radius of GCs (= 3 pc).

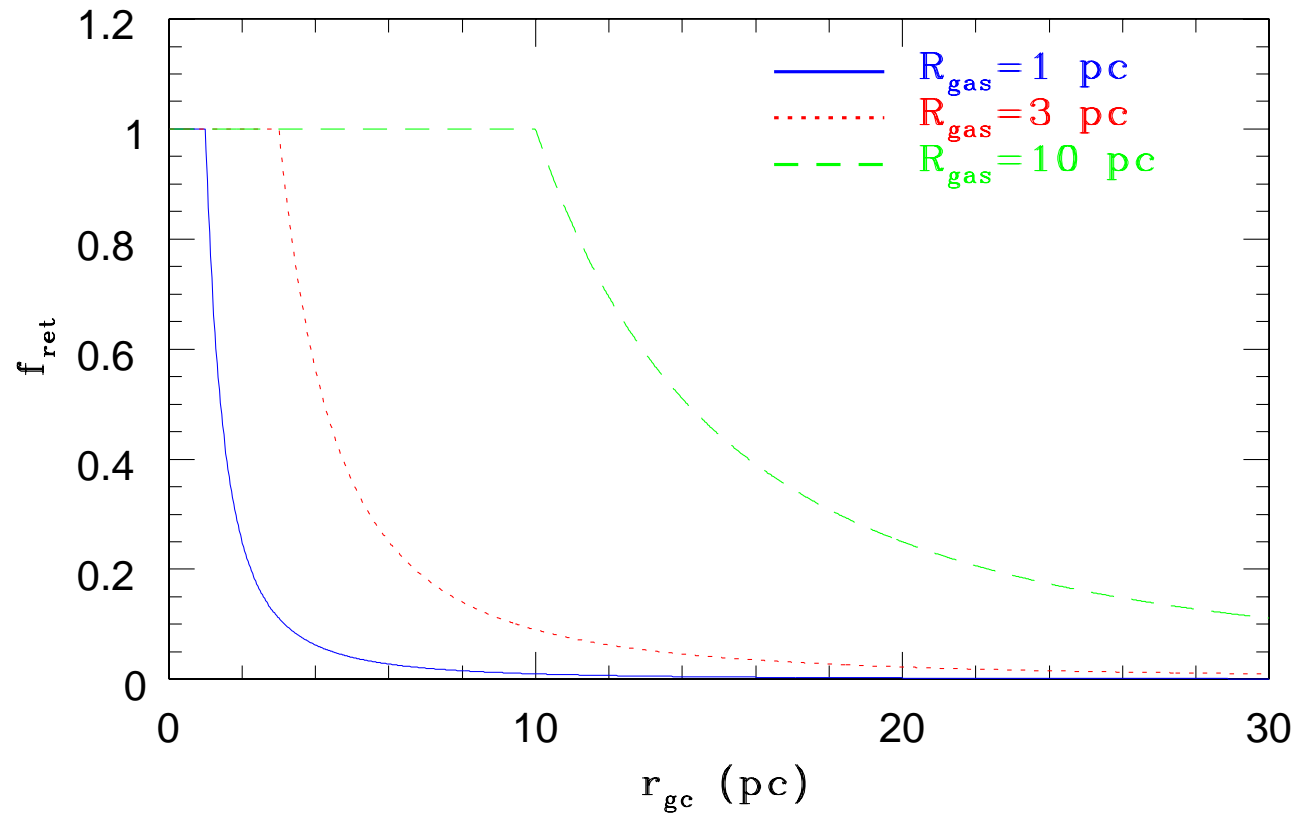


FIG. 3.— Return fraction of NSM ejecta (f_{ret}) as a function of the distance between the location of an NSM and the center of a GC (r_{gc}) for $R_{gas} = 1$ pc (blue solid), 3 pc (red dashed), and 10 pc (green short-dashed). Since l_s is very small (< 10 pc), the ejecta from a NSM within R_{gas} is assumed to be all trapped by AGB ejecta in this figure.

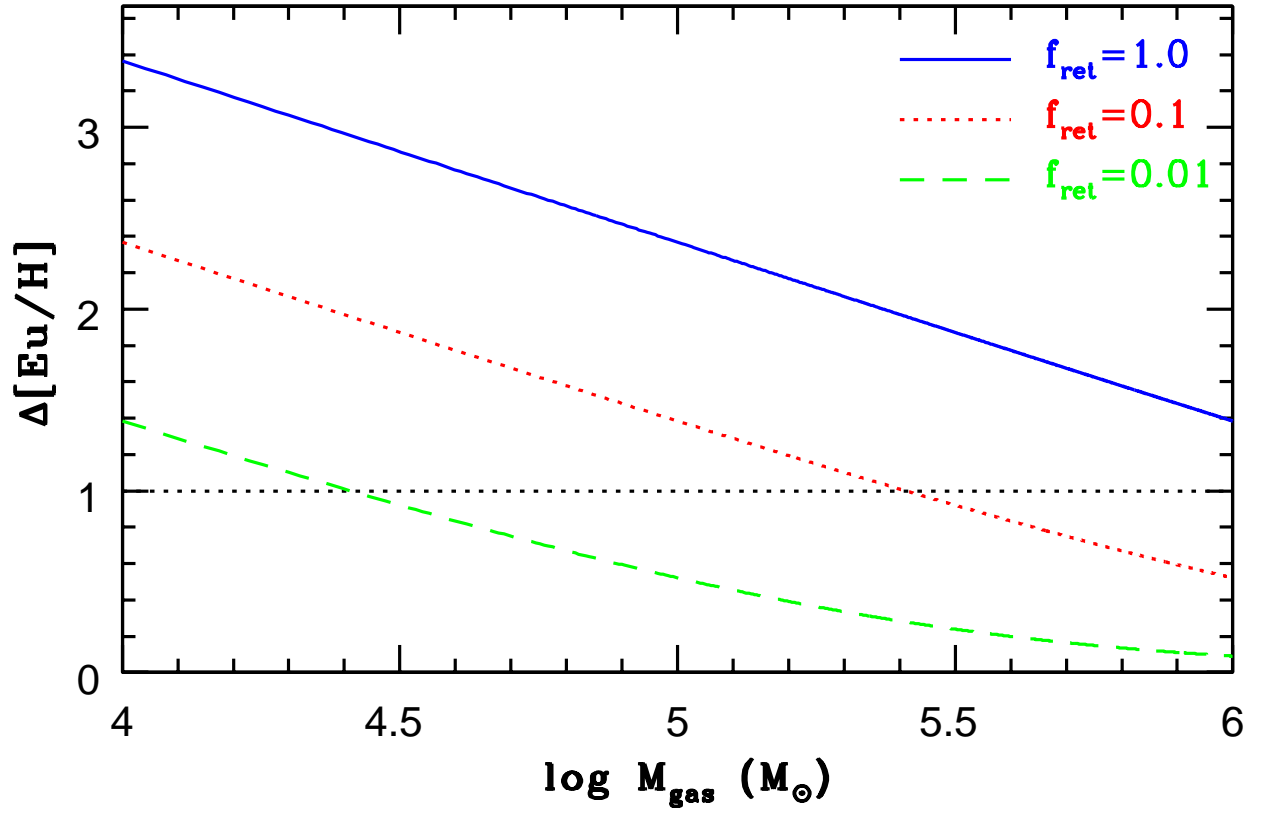


FIG. 4.— Internal spread of $[\text{Eu}/\text{H}]$ ($\Delta[\text{Eu}/\text{H}]$) as a function of M_{gas} for $f_{\text{ret}} = 1.0$ (blue solid), 0.1 (red dashed), and 0.01 (green short-dashed). The black dotted line indicates the observed ($\Delta[\text{Eu}/\text{H}]$) for M15 (W13).

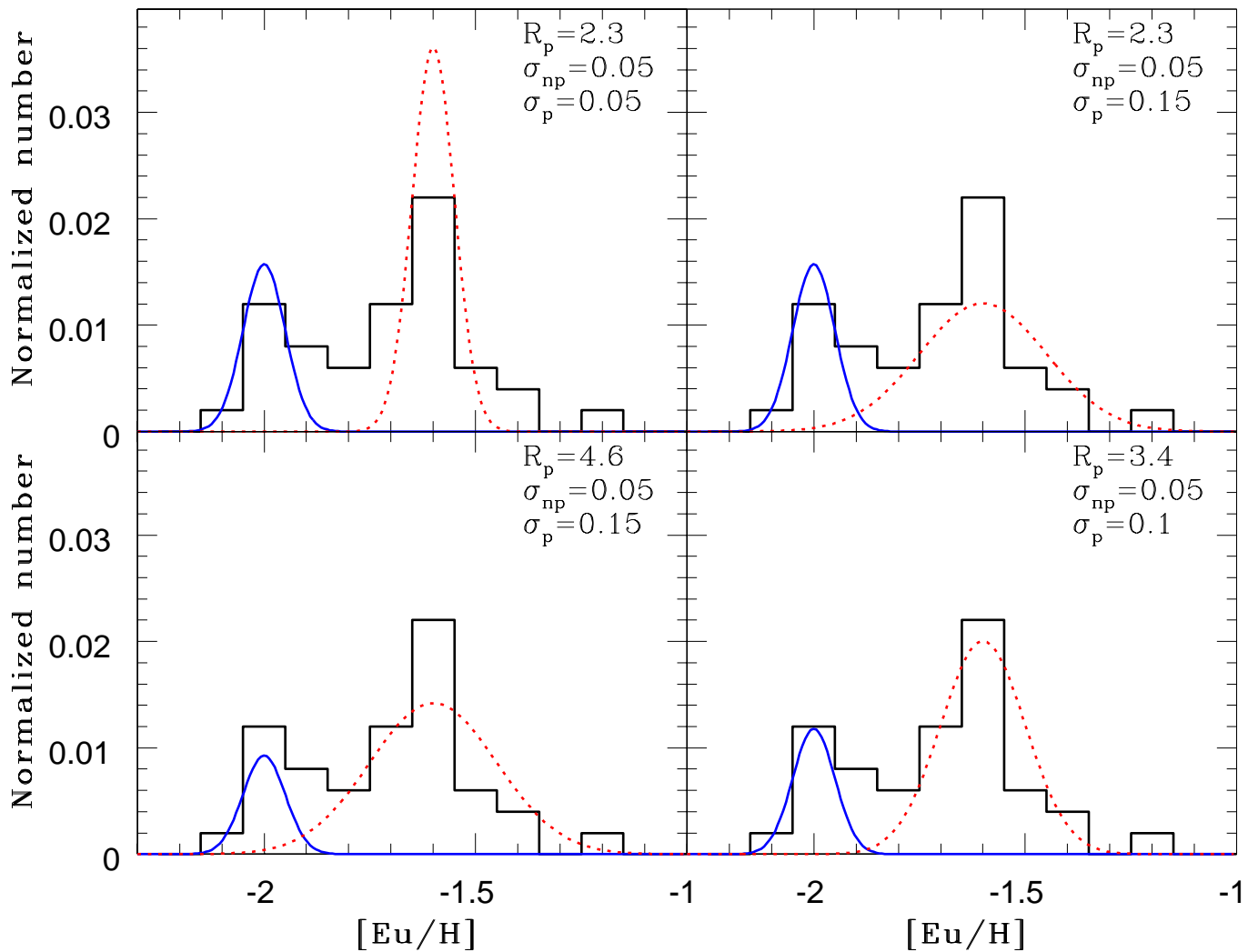


FIG. 5.— Normalized distribution of $[\text{Eu}/\text{H}]$ for the four representative models with different R_p (number ratio of polluted stars to non-polluted ones), σ_{np} ($[\text{Eu}/\text{H}]$ dispersion for non-polluted stars), and σ_p ($[\text{Eu}/\text{H}]$ dispersion for polluted stars). These values of the parameters are given in the upper right corner of each panel. The blue solid and red dotted lines indicate stars formed from gas not being polluted by NSM ejecta and those formed from gas polluted by the ejecta, respectively. The thick black line in each panel describes the observed (normalized) distribution of $[\text{Eu}/\text{H}]$.

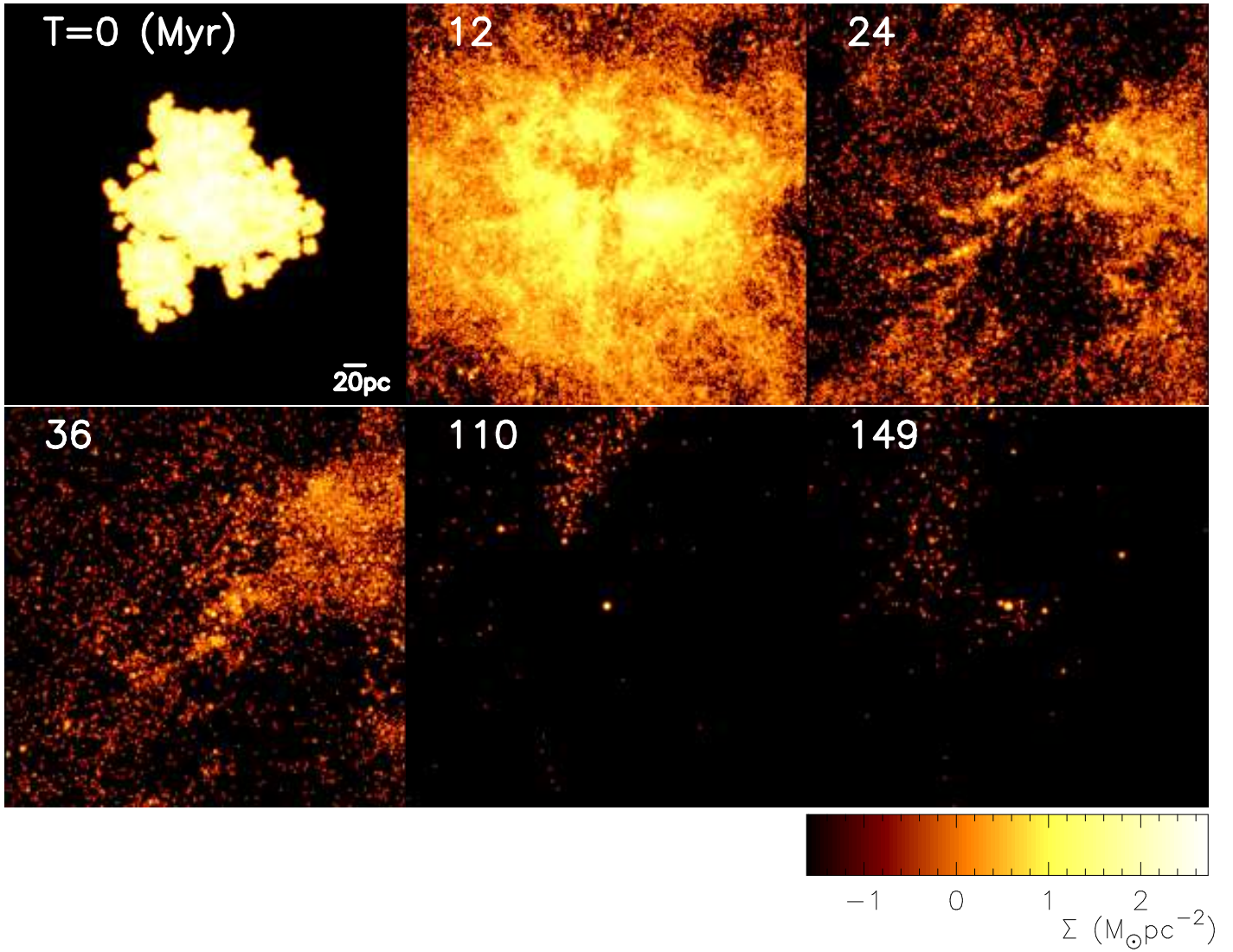


FIG. 6.— Time evolution of the gas density (Σ) of a GC-forming molecular cloud (MC) projected onto the x - y plane for the model M1. Time T (in units of Myr) is indicated in the upper left corner of each panel. The gas density is given in a logarithmic scale.

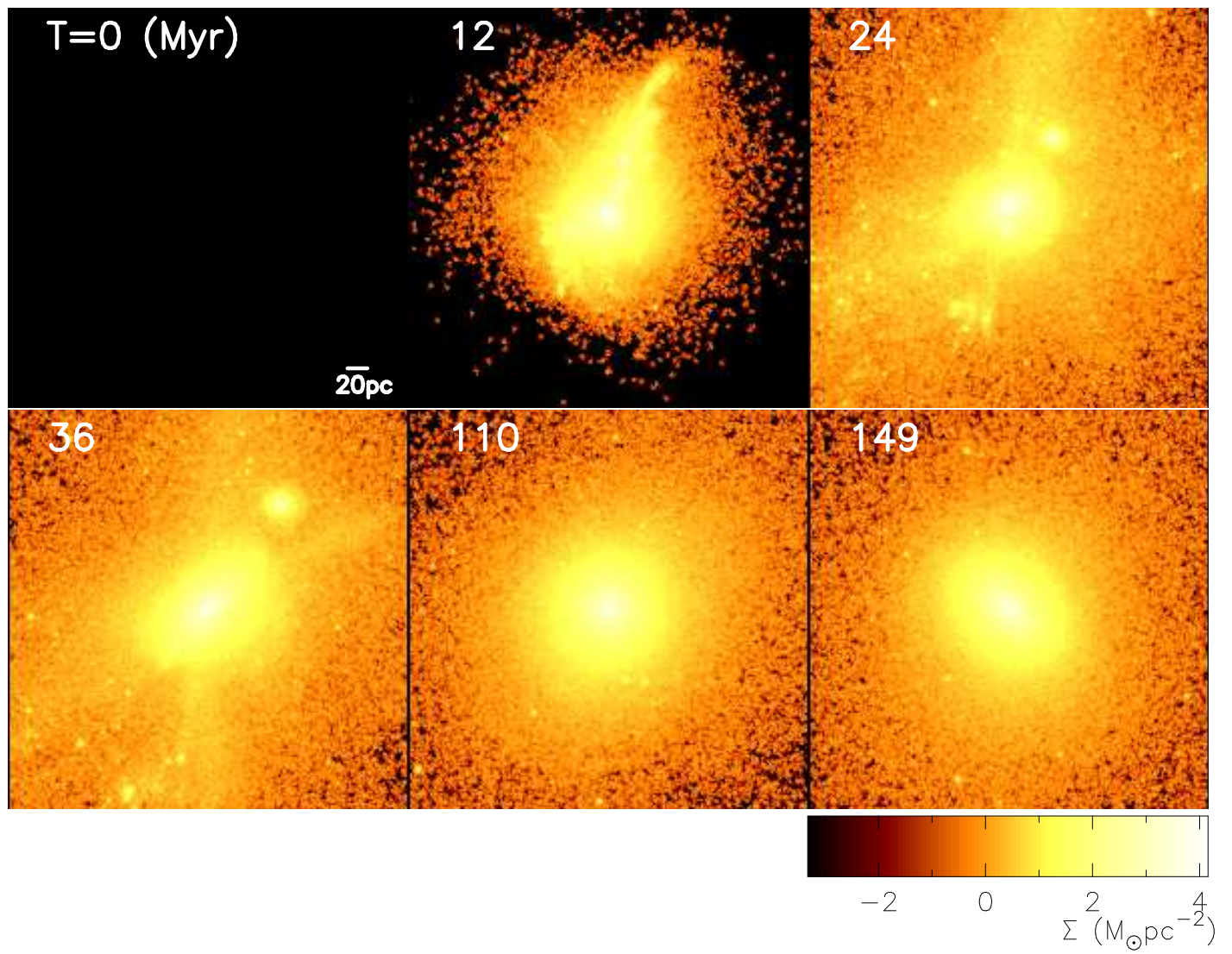


FIG. 7.— The same as Fig. 6 but for the new stars formed from the initial gas of the MC.

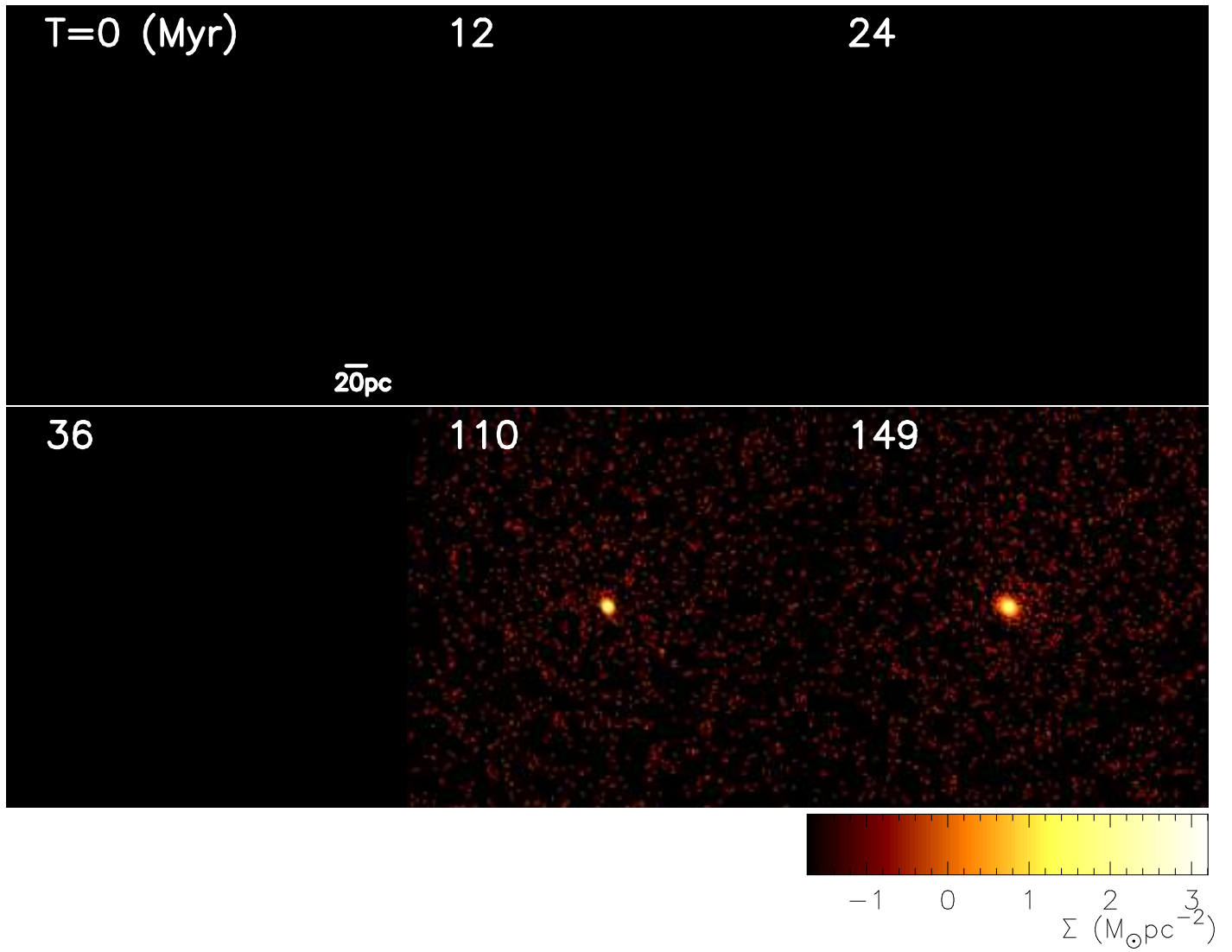


FIG. 8.— The same as Fig. 6 but for the gas ejected from AGB stars. It is clear that a very high-density compact gaseous region is formed in the central region from AGB ejecta at $T = 110$ and 149 Myr.

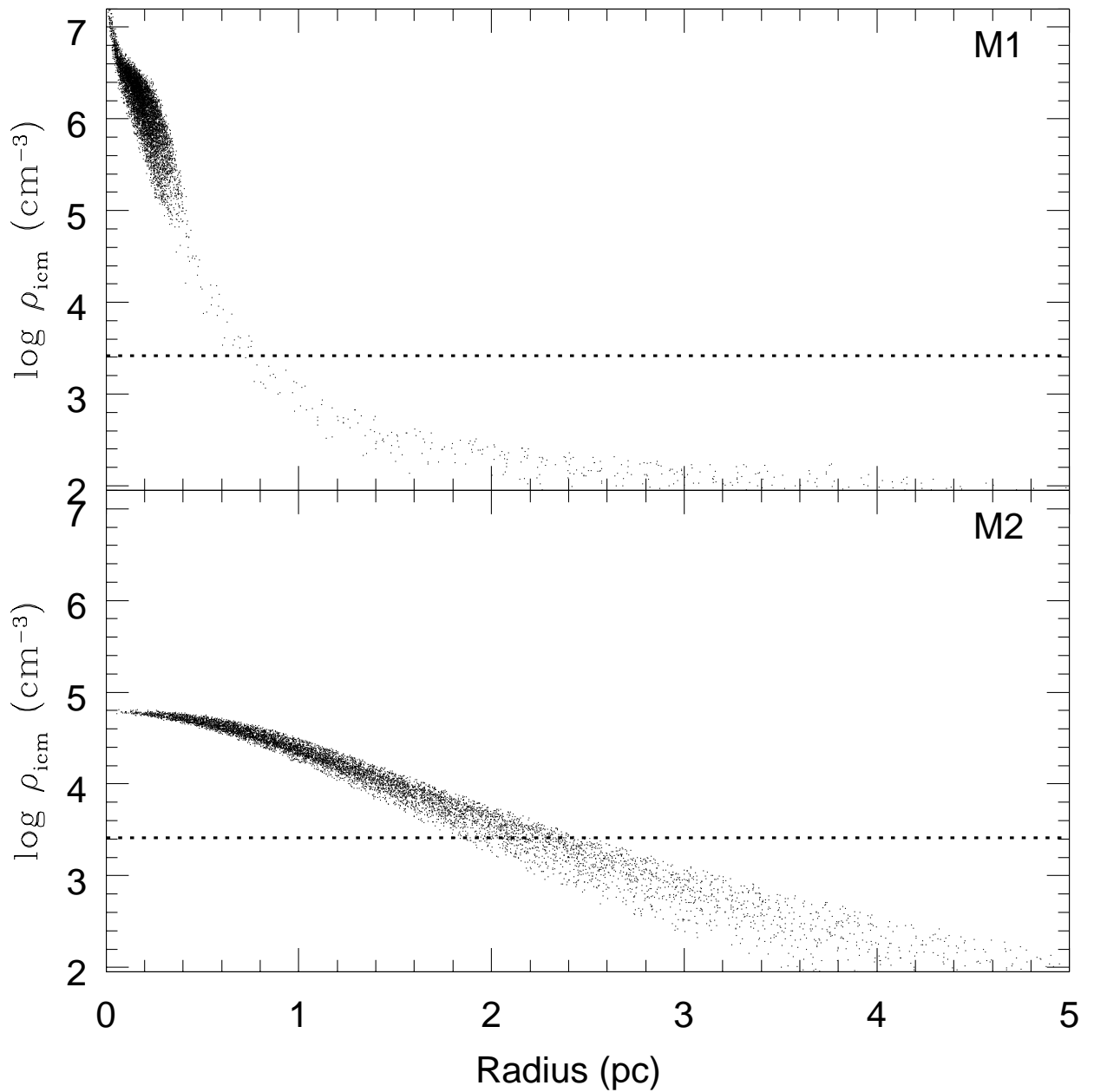


FIG. 9.— Radial distribution of the mass density of the intra-cluster medium (ICM; ρ_{icm}) for M1 (upper) and M2 (lower). Each small dot indicates the location and ρ_{icm} of each gas particle on this plot. A horizontal dotted line in each frame indicates ρ_{icm} above which NSM ejecta can be stopped through interaction with the ICM. M1 and M2 are the GC formation models without and with secondary star formation, respectively.

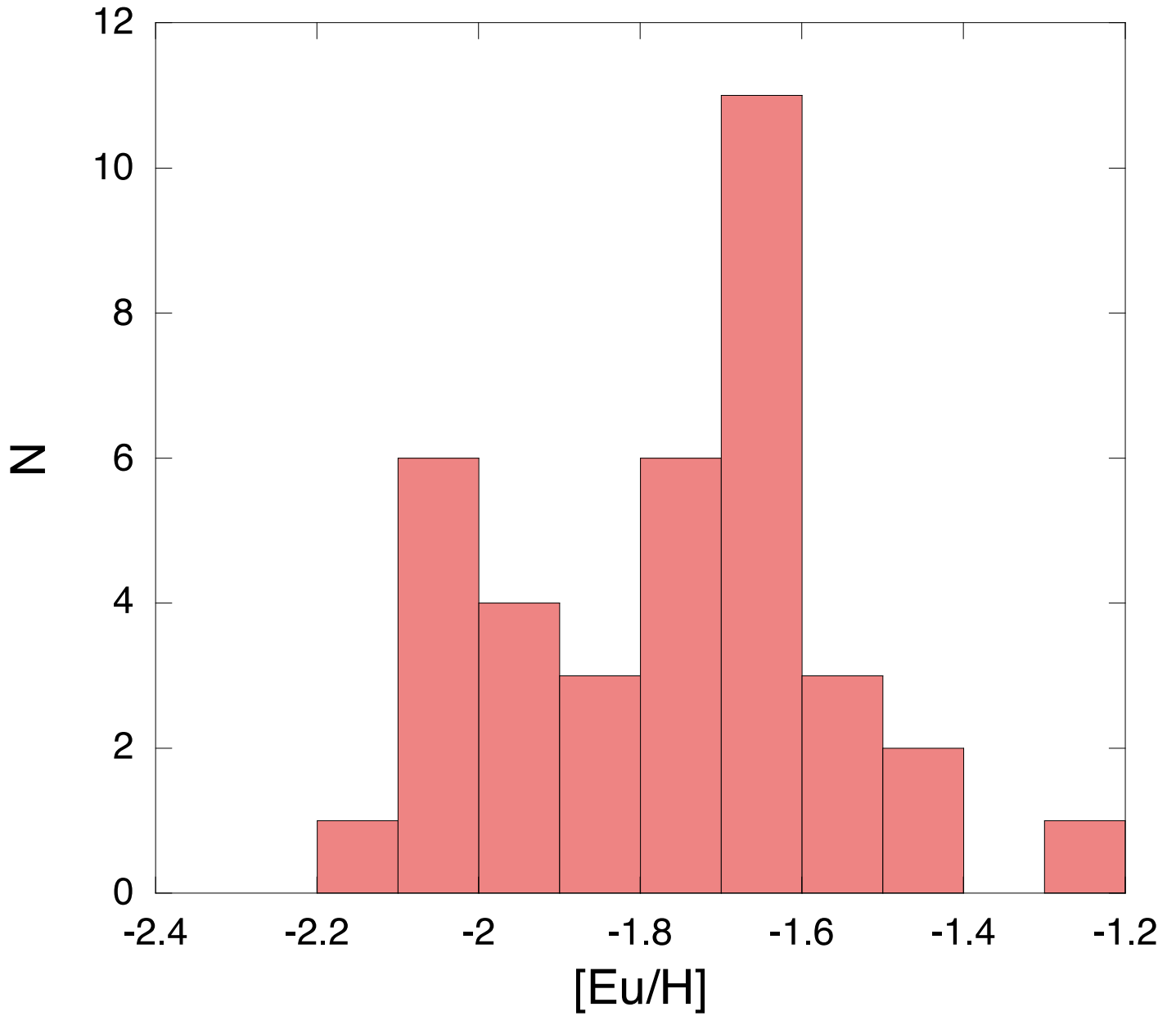


FIG. A10.— [Eu/H] distribution of M15 reproduced from observational data by W13 and S11. Clearly, there are two peaks around [Eu/H]=-2.0 and -1.6 in the distribution.

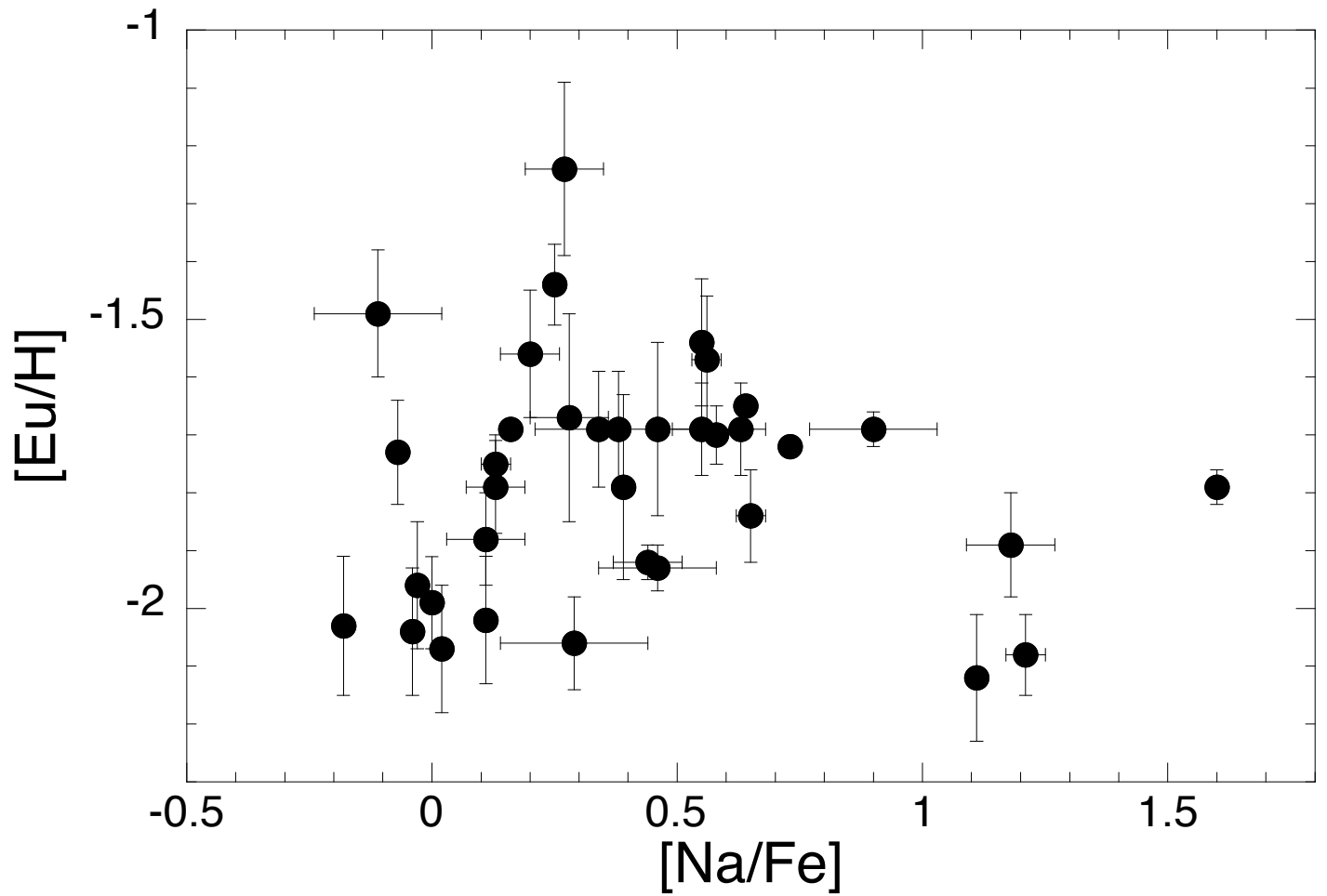


FIG. A11.— $[\text{Eu}/\text{H}]$ of stars as a function of $[\text{Na}/\text{Fe}]$ in M15. This plot is reproduced from the observational data by W13 and S11.